scientific data

OPEN

DATA DESCRIPTOR

Kinematics, kinetics, and muscle activations during human locomotion over compliant terrains

Charikleia Angelidou, Vaughn Chambers, Bradley Hobbs, Chrysostomos Karakasis & Panagiotis Artemiadis ✉

Walking on compliant terrains, like carpets, grass, and soil, presents a unique challenge, especially for individuals with mobility impairments. In contrast to rigid-ground walking, compliant surfaces alter movement dynamics and increase the risk of falls. Understanding and modeling gait control across such soft and deformable surfaces is thus crucial for maintaining daily mobility. However, access to the necessary equipment for modeling compliant surface walking is limited. Therefore, in this paper, we present the first publicly available biomechanics dataset of 20 individuals walking on terrains of varying compliance, using a unique robotic device, the Variable Stiffness Treadmill 2 (VST 2), designed to simulate walking on adjustable compliant terrain. VST 2 provides a consistent and reproducible environment for studying the biomechanics of walking on such surfaces within laboratory settings. The goal of this dataset is to provide insights into the muscular, kinematic, and kinetic adaptations that occur when humans walk on compliant terrain in order to design better controllers for prosthetic limbs, improve rehabilitation protocols, and develop adaptive assistive devices that can enhance mobility on compliant surfaces.

Background & Summary

Given the importance and frequency of walking in human life, understanding and modeling gait is crucial. Even in a controlled environment with level, rigid ground, and no external perturbations, gait modeling is complex and does not fully replicate the challenges of traversing in the real world. To develop effective rehabilitation strategies for paretic gait and advanced controllers for robotic walkers and prosthetic and wearable technologies, we must understand and model gait control across various environments[1].

Walking on compliant terrain poses a unique challenge and is a critical aspect of daily mobility for many individuals. Compliant terrains include soft and deformable surfaces found both indoors and outdoors, such as carpets, grass, and soil[2]. Unlike walking on rigid and stable surfaces, compliant terrains can shift underfoot and disrupt normal movement dynamics, significantly impacting walking stability and increasing the risk of falls in humans[3–5]. Understanding the dynamics of walking on such surfaces is therefore essential, particularly for those with mobility impairments, such as people with lower limb amputations[6] and stroke survivors[7], who often find navigating these terrains significantly more challenging. Individuals with lower-limb amputations, for instance, face difficulties due to the lack of proprioceptive feedback from the missing limb and the altered biomechanics introduced by prosthetic devices[8]. These challenges are exacerbated on compliant surfaces, where the instability can lead to increased energy expenditure and a higher risk of falls[9]. Previous works specifically report lower walking speeds and increased step width, step time asymmetry, and variability for people with transfemoral amputation when walking over compliant terrains[10], as well as decreased postural stability for individuals with transtibial amputation when standing on a compliant foam surface[11]. Similarly, stroke survivors often deal with hemiparesis, which affects muscle strength and coordination on one side of the body, making it harder to adapt to the irregularities and demands of compliant terrains[7]. Other populations, such as the elderly or those with neuromuscular disorders, also struggle with maintaining balance and stability on these surfaces, which can impact their independence and quality of life[12]. At the same time, compliant tracks have led to improved performance for runners, while decreasing the occurrence of injuries[13]. Compliant terrains, therefore, constitute a unique type of terrain with variable effects for different populations.

University of Delaware, Department of Mechanical Engineering, Newark, DE, 19716, USA. ✉e-mail: partem@udel.edu

ID	Gender	Age	Height (m)	Body Mass (kg)	Leg Length (m)	Resting HR (bpm)	Preferred Speed (m/s) Rigid	Preferred Speed (m/s) Compliant 3
01	Male	26	1.78	75.5	840	68	1	0.9
02	Female	27	1.65	70.8	840	58	0.975	0.875
03	Female	28	1.63	64.9	805	65	0.95	0.95
04	Female	29	1.73	68	840	58	0.95	0.85
05	Male	36	1.77	85.6	780	60	1.05	0.9
06	Male	19	1.77	72.5	860	65	0.875	0.8
07	Female	37	1.63	64.6	810	75	0.9	0.95
08	Male	27	1.89	86.8	930	75	1	1
09	Male	26	1.80	76	920	50	0.95	0.95
10	Male	28	1.74	78	780	67	0.95	0.9
11	Female	24	1.68	58.9	870	63	0.95	0.9
12	Female	29	1.70	69.4	830	67	0.95	0.9
13	Female	21	1.68	60.1	810	61	1	0.9
14	Male	25	1.75	60	860	65	0.95	0.9
15	Male	25	1.70	55.3	860	47	1.05	1.1
16	Female	32	1.75	89	900	75	0.95	0.8
17	Female	30	1.75	59	880	84	0.9	0.875
18	Male	24	1.65	81	800	78	0.9	0.8
19	Female	22	1.65	81.2	830	78	1	0.95
20	Male	26	1.78	82.9	930	72	0.95	0.9

Table 1. Demographic and anthropometric information of the participants.

Despite the critical need to understand and improve mobility on compliant surfaces, research in this area is limited, focusing on a restricted number of study variables[14,15] or on isolated patient populations[16]. Although more recent works have delved deeper into the effects of compliant terrains, thoroughly studying walking stability[17,18], muscle activations and gait kinematics[19–22], gait on compliant surfaces has not received the same level of attention as rigid ground walking, which has been extensively investigated[23–25]. The resources to study gait over rigid surfaces, unlike compliant surfaces, are also ample, with the existence of a series of open-source datasets related to various activities of daily living[26–29].

This paper addresses this gap by introducing the first open-source dataset on compliant terrain. In this dataset we report kinematic, kinetic, and electromyographic (EMG) data from 20 healthy individuals while walking on terrains of varying compliance. These terrains are realized using a unique robotic device, the Variable Stiffness Treadmill 2 (VST 2)[30], specifically designed to simulate walking on adjustable compliant terrain. VST 2 allows researchers to simulate walking on various compliant surfaces within a controlled laboratory setting. By adjusting the stiffness of the treadmill surface, VST 2 can mimic different types of terrain, providing a consistent and reproducible environment for studying the biomechanics of walking on such surfaces.

The significance of this dataset lies in its potential applications and the contribution it offers to the field. Researchers can use this dataset to gain insights into the muscular, kinematic and kinetic adaptations that occur when humans walk on compliant terrain. For example, the data can be used to identify specific gait patterns, balance strategies, and muscle activation profiles that individuals adopt over compliant surfaces. This information is crucial for designing better controllers for prosthetic limbs, improved rehabilitation protocols, and adaptive assistive devices that can enhance mobility on compliant surfaces, as well as for optimizing controllers for robotic walkers.

This work presents a valuable resource, facilitating comparisons and meta-analyses that can drive the field of robotic locomotion, prosthetics, and rehabilitation forward. By leveraging VST 2 to simulate compliant terrain in a controlled environment, we provide a reproducible dataset that addresses a critical gap in the study of human gait, as well as paves the way for practical applications that can improve the quality of life for many.

Methods

This section outlines the procedure from obtaining participant consent to acquiring and processing the data for publication. Each section proceeds step-by-step through the procedure and details the completed trials.

Participants. The participants were formally recruited and selected based on the following inclusion criteria: (i) healthy gait; (ii) age over 18 years; (iii) body mass between 50 and 90 kg; and (iv) height between 1.50 and 1.90 m. Participants reported no lower-extremity injuries in the six months before data collection and did not have any musculoskeletal or neurological conditions affecting their ability to walk or balance. These criteria ensured a dataset with a stratified anthropometric distribution, while taking into account potential gender biomechanical differences[31]. Consequently, twenty healthy participants (10 males and 10 females) were involved in the study (average age 27.1 $\pm$ 4.5 years, average height 172.4 $\pm$ 6.8 cm, average weight 68.4 $\pm$ 12.2 kg) (see Table 1). A pilot study was conducted with one participant to refine the experimental procedures for this study. Prior to

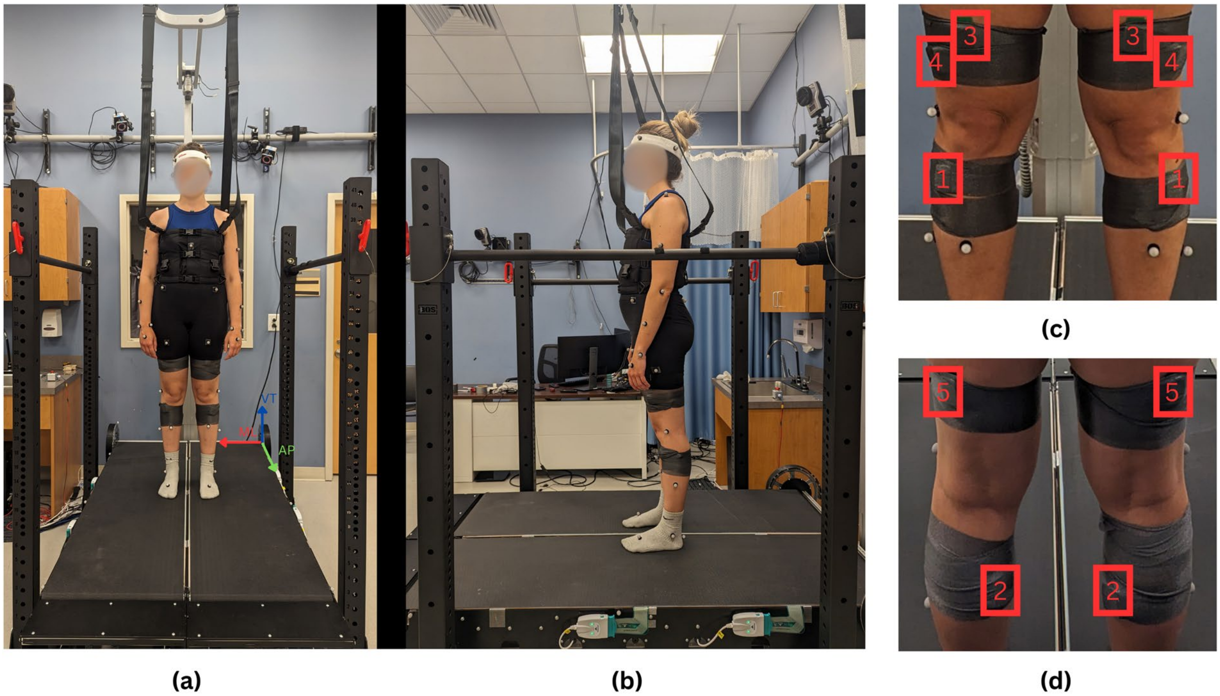

Fig. 1 Front (**a**), and side (**b**) view of the setup showing a representative participant standing on the Variable Stiffness Treadmill 2 (VST 2). The participant is fully instrumented with 43 reflective markers and 10 EMG sensors attached to the participant's skin, shown on the (**c**) and (**d**) subfigures: (1) - TA, (2) - GA, (3) - RF, (4) - VL, and (5) - BF. Six additional markers were placed on the front, middle, and back edges of both VST 2 belts to monitor belt deflection at all times. All participants wore a bodyweight support harness that did not offset any weight but was used for safety.

data collection, each participant reviewed and signed a consent form approved by the University of Delaware Institutional Review Board (IRB ID# 1544521-8).

Instrumentation and participant preparation. Data were acquired at the University of Delaware Science, Technology and Advanced Research (STAR) Campus. The laboratory where data collection took place is equipped with a motion capture system and a unique, instrumented split-belt treadmill that can simulate walking on compliant terrains. We recorded the kinematics, kinetics, and muscular activations of walking on compliant surfaces. Synchronous data acquisition was managed by the Vicon motion capture system for the kinematic and EMG data, while more information about data synchronization is provided in the Data Processing Section.

Participant preparation. The participants were equipped with surface EMG electrodes and a set of full-body motion capture markers as illustrated in Figs. 1 and 2. The participants were asked to wear tight-fitting, non-reflective clothing. Cohesive wraps were used when necessary to ensure the clothing stayed tight to the skin. Markers were placed at all required locations for the Vicon plug-in Gait Full-body model[32], along with a custom set of additional markers on our split-belt treadmill to capture the deflection of the belts. A comprehensive description of the markers and their placement is provided in Fig. 2. Overall, 49 reflective markers were utilized. The Plug-In Gait markers were placed directly on the skin, on the tight-fitting clothes of each participant, and on the harness that all volunteers were required to wear throughout the experiment for safety purposes.

A 10-channel wireless surface EMG system (Trigno - Delsys, Massachusetts, USA), sampling data at 2000 Hz, recorded Inertial Measurement Unit (IMU) data and EMG signals from five lower limb muscles including the tibialis anterior (TA), gastrocnemius (GA), rectus femoris (RF), vastus lateralis (VL), and biceps femoris (BF), of both legs, as depicted in Fig. 1. Before placing the EMG sensors on the participants, the skin above each muscle was shaved to remove any hair affecting the contact of the electrode and was subsequently gently cleaned using alcohol wipes. Once cleaned, the EMG electrodes were attached to the skin with double-sided adhesive tape. Variability was reduced by following SENIAM guidelines[33,34]. To prevent EMG sensor displacement during data acquisition, each sensor was secured with medical tape (see Fig. 1), ensuring reliable measurements without introducing errors. After each sensor placement, the subjects were asked to contract the corresponding muscle to ensure that a viable location was found, and a low signal-noise ratio was achieved. In this way, the quality of all EMG signals was assessed, and sensor placement was adjusted as necessary.

All participants were asked to walk wearing only their socks to ensure consistency across trials, as wearing shoes could alter their interaction with the walking surface, thereby affecting the force interaction with the treadmill environment. A heart rate monitor (Polar H10) worn around the chest and directly on the skin recorded the participants' heart rate at a 1 Hz frequency. Body weight support (BWS) was set to 0%, and participants were

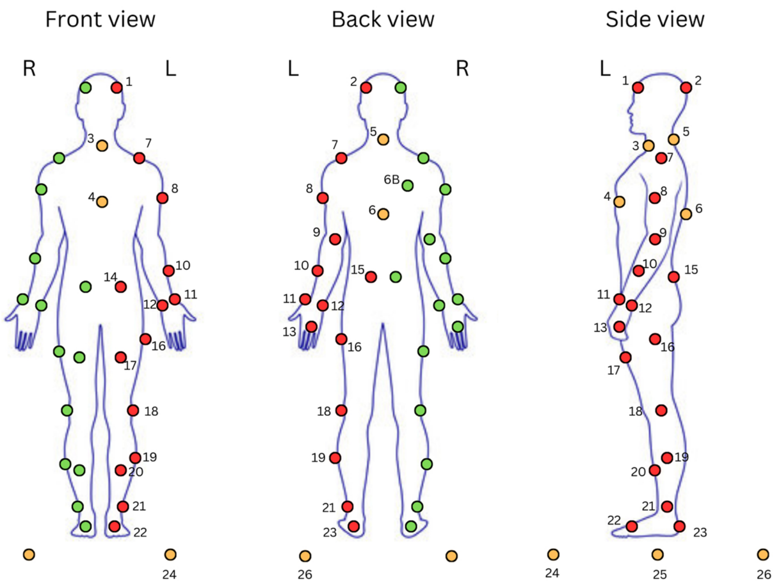

Marker set	#	Side	Code	Anatomical Description
Upper Body marker Set	1	L/R	FHD	Front Head
	2	L/R	BHD	Back Head
	3	-	CLAV	Clavicle
	4	-	STRN	Sternum
	5	-	C7	7th Cervical Vertebra
	6	-	T10	10th Thoracic Vertebra
	6B	R	BAK	Back
	7	L/R	SHO	Shoulder
	8	L/R	UPA	Upper arm
	9	L/R	ELB	Elbow
	10	L/R	FRM	Forearm
	11	L/R	WRA	Wrist Marker A
	12	L/R	WRB	Wrist Marker B
	13	L/R	FIN	Finger
Lower Body marker Set	14	L/R	ASIS	Anterior Superior Iliac Spine
	15	L/R	PSIS	Posterior Superior Iliac Spine
	16	L/R	THI	Thigh
	17	L/R	THIA	Anterior Thigh
	18	L/R	KNE	Knee
	19	L/R	TIB	Tibia
	20	L/R	TIBA	Anterior Tibia
	21	L/R	ANK	Ankle
	22	L/R	TOE	Toe
	23	L/R	HEE	Heel
VST	24	L/R	Belt1	Front Belt Marker
	25	L/R	Belt2	Middle Belt Marker
	26	L/R	Belt3	Back Belt Marker

Fig. 2 Locations and names of the markers in the modified Plug In Gait Full Body model[32]. Markers were placed symmetrically left (red) and right (green), therefore, only the left side markers are labeled. The treadmill belt markers were added to Vicon's Plug In Gait Full Body model and are presented in orange.

instructed to walk without holding onto the treadmill rails unless they encountered any safety or balance-related issues. However, no such issues occurred during any of the twenty trials.

Motion capture. An 8-camera Vicon motion capture system (Vicon, Oxford, UK) was used to record the 3D positions of all markers attached to participants at 100Hz. Vicon's Plug-in Gait Full-body model was employed to calculate joint angles from markers positions. The joint angular conventions, alongside further information on the Plug-in Gait kinetic modeling, are available in the Nexus Plug-in Gait Reference Guide[32]. The cameras of the motion-capture system were calibrated according to the manufacturer's instructions within the capture volume[35]. The volume origin was set using three reflective markers attached to the bottom frame of the treadmill (see Fig. 1).

After obtaining informed consent and preparing the participants' marker set (see Fig. 2), the participants were instructed to stand still for a static calibration of the marker set. During the calibration, participants were standing on the treadmill with their arms spread out at shoulder height, forming a T-shape, looking forward, and with the feet in a comfortable position, aligned with the shoulders. The necessary marker position adjustments were addressed during the static calibration and before proceeding with the experiment trials.

Variable Stiffness Treadmill 2 (VST 2). All participants were asked to walk on VST 2, a unique split-belt treadmill with a walking surface that can change the vertical compliance of its belts. The first iteration of this device, VST 1, was the first treadmill capable of altering vertical ground stiffness[36,37]. The second and enhanced iteration of the split-belt treadmill, VST 2, was recently developed and used for the purposes of this study[30]. VST 2 is capable of independently altering the stiffness of both belts within a range of 13 kN/m to 1.5 MN/m, to simulate walking on soft surfaces. The speed of the belts is also independent, as each belt has a dedicated motor. With its high accuracy and precision, along with additional upgrades and features, such as its large walking surface that allows for comfortable walking or running, VST 2 stands out as a unique device with significant research potential. Its capability for bilateral stiffness and velocity control enables the collection and analysis of gait data that were previously unattainable with other devices, such as the center of pressure path, vertical ground reaction forces, and surface deflection from both legs while walking on compliant surfaces, to name a few. The treadmill was remotely controlled by a custom code developed by our lab, as part of the development of VST 2, to change the belt speed and stiffness across and within trials. The acquisition of the force data, including the vertical ground reaction forces and foot center of pressure, is based on high-spatial resolution force mats installed underneath both treadmill belts[30]. The embedded force plates under each belt acquire kinetics independently for each leg at 65 Hz.

Experimental Procedure. This dataset captures the kinematics, kinetics, and muscle activations of human gait during walking on rigid terrain and on surfaces of varying compliance. The primary goal of this work is to provide a comprehensive collection of data for modeling human biomechanics over surfaces of different stiffness. Therefore, our study focuses on the changes in the surface stiffness and how they affect human gait under different speeds. Including multiple treadmill speeds as an independent study variable in this dataset can provide insights into the locomotion patterns over compliant terrain at various speeds, however, as noted before, this study does

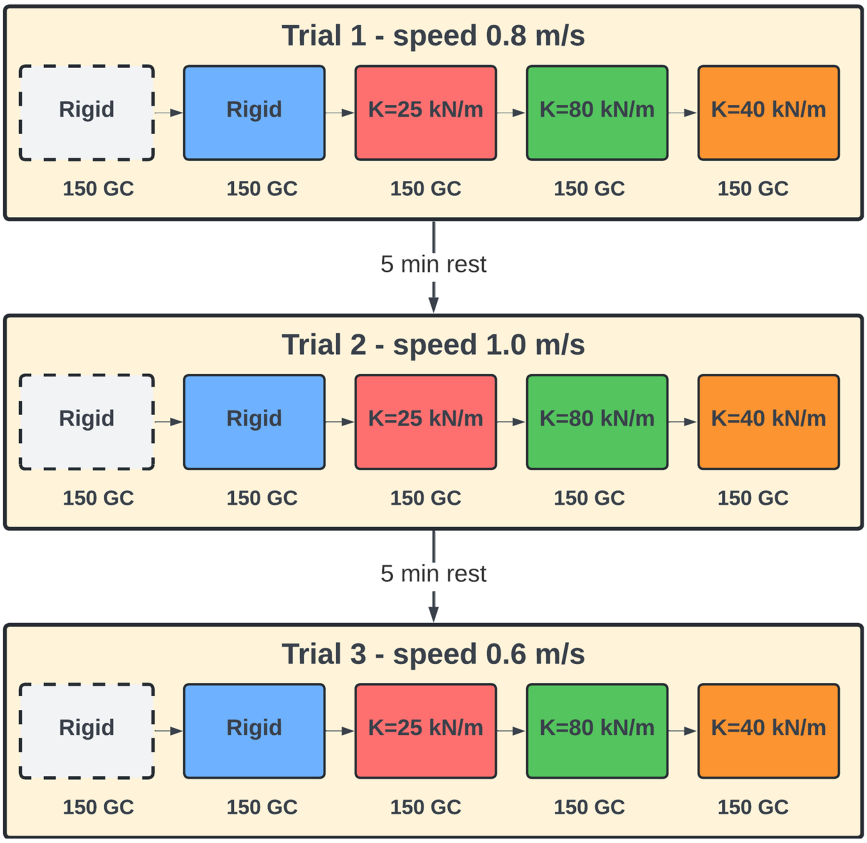

Fig. 3 Data acquisition workflow. Each condition was tested for 150 gait cycles. The first 150 gait cycles of each trial served as force mat warm-up time. Participants were unbuckled from the safety harness between trials to rest for 5 minutes before proceeding to avoid fatigue.

not extensively focus on the effect of speed. For this reason, only three different, pre-defined speeds were evaluated. For each of these three different speeds, four different values of belt stiffness were tested, each one lasting for 150 gait cycles. The entire process and sequence of conditions are described in Fig. 3.

Four different stiffness levels and three different walking speeds were tested, accounting for a total of 12 conditions. Data for 150 gait cycles were recorded for each condition. For reference purposes, each gait cycle is defined as starting and ending at consecutive left heel-strikes. The experimental procedure included a familiarization phase prior to data collection where participants walked on VST 2, identified their preferred walking speed, acclimated to the different speeds, and also shortly experienced the stiffness levels included in the analysis to avoid surprises during the actual experiment. For all participants, we recorded and reported their comfortable walking speed over rigid ground, as well as over the most compliant treadmill setting that was tested. All reported speeds were within the range of 0.8-1 m/s (with the sole exception of participant ID#15, who reported himself as a runner) (see Table 1). Individuals in this study selected, on average, a slower walking speed for the most compliant surface case compared to rigid surface walking.

In our experimental protocol, we included three speeds, namely 0.6 m/s, 0.8 m/s, and 1.0 m/s. This range was found suitable, since the relatively low speed of 0.6 m/s accounts for the preferred treadmill speeds reported by individuals with gait impairments (e.g., individuals with lower-limb amputation or stroke survivors)[38], while the higher speeds tested account for self-reported speeds during average, healthy walking on our treadmill[20] (see Table 1). A 0.2 m/s increment was selected to ensure participants could discern the difference between speeds effectively.

The four treadmill stiffness levels tested are presented in Table 2. The Rigid setting constitutes the baseline condition, which other datasets have extensively studied, and the three compliant surface conditions (high, medium, and low stiffness) are compared against it.

For each participant, the entire data collection was acquired in a single session, which lasted approximately 2.5 hours. All the sessions were managed by the same experienced operator. Each experiment consisted of 3 trials, corresponding to the three different speeds that were tested. The speed was, therefore, kept constant throughout a single trial, while the surface stiffness would change every 150 steps following the pre-defined order described in Fig. 3. Each trial had a total duration of approximately 12-20 minutes depending on the trial speed and characteristic gait patterns of each individual (i.e., step length, gait cycle duration). Between trials, participants were unbuckled from the safety harness and were allowed to sit for a 5-minute break. The reported resting heart rate (HR) measurements were acquired during the first break between trials, while the participants were relaxed and seated. A schematic overview of the data collection sequence is provided in Fig. 3.

	VST 2 Stiffness Value K (kN/m)			
	Rigid	High Stiffness	Medium Stiffness	Low Stiffness
Desired	1000	80	40	25
Actual (avg)	∞	89.43	41.31	27.21
Actual (std)	—	5.90	2.43	1.64

Table 2. Desired and actual VST 2 belt stiffness. The desired stiffness corresponds to the stiffness command that was sent to the variable stiffness mechanism (VSM) of VST 2. The actual stiffness corresponds to the average calculated stiffness of both belts across all participants during the peak stance phase of each gait cycle (max. belt deflection) in a single trial (trial 1: speed 0.8 m/s). The standard deviation shows the stiffness value variation per condition.

The progression of tested speeds and stiffness changes between participants remained the same for ease of acquisition and consistent data processing, especially for the transition steps between conditions.

Data Processing. Following data collection, the 3D trajectories for each of the reflective markers were fully reconstructed and labeled. Once the markers were labeled, gaps in the marker trajectories were filled using rigid-body, spline, and pattern fill algorithms[35]. Specifically, first, a Woltring filter was used for gaps equal to or less than 0.05 *s*. Next, a rigid-body filter was used, which employed proximal markers on the same body segment to fill gaps equal to or less than 0.25 *s*. The remaining gaps were filled with the Vicon Nexus 2.16 kinematic filter[35].

A custom MATLAB script was implemented to process and synchronize all data, parse trials into stiffness conditions, parse conditions into gait cycles, and compile everything into a unified MATLAB structure. The MATLAB processing framework included the following processes.

Data synchronization was ensured in a few different ways. A Delsys trigger module (Delsys Inc.) ensured synchronization of the EMG data with the markers and kinematics streamed from Vicon. A data acquisition device (USB 6008, National Instruments Corporation) ensured Ground Reaction Force (GRF) data was synchronized with VST 2, and a high-speed TCP/IP connection ensured synchronization between the motion capture data and VST 2. Timestamps of the force, heart rate, and VST 2 data were collected and then utilized for synchronization purposes. It is important to note that the recorded, timestamped VST 2 data included the left and right heel marker data, which were directly streamed from Vicon. Subsequently, the Vicon captured data and muscle activity data were synchronized with the timestamped data (force, heart rate, and VST 2) by matching marker values. Any excess data recorded from the VST 2, force mats, and heart rate monitor were trimmed off to match the Vicon data using the same strings of marker data found in both datasets at the start and end of the experiment. Finally, force, heart rate, and VST 2 data were resampled to 100 *Hz* using linear interpolation to agree with the Vicon data, which was recorded at 100 *Hz*. For reference, the average inter-participant kinematic profiles, the average normalized heart rate data for the middle speed (0.8 m/s), and the average deflection of the VST 2 belts across participants are presented in Fig. 4, Fig. 5, and Fig. 6 respectively. It should be noted that in this dataset, included are the resampled heart rate and VST 2 data, however, the rest of the recorded data, including the EMG and force data, are provided in their raw form.

Force data was captured using force mats (TekScan 3140 with VersaTek Cuffs, TekScan Inc.), which are located between the treadmill belts and the wooden surface that supports the belts. These mats collect force data with a spatial resolution of 1 *cm* in both the anterior/posterior and medial/lateral directions. There are 4224 force-sensing cells on each treadmill belt. From these sensors, the total force applied can be calculated by summing up all the force cells measurements, as well as the location of the center of pressure (CoP) using the positions of the cells when averaging the measured forces. An indicative representation of the CoP data captured by the force mats is also presented in Fig. 7. Force data was captured at 65 *Hz* and then filtered with a moving average filter with a window size of 60 data points to reduce high-frequency noise and fluctuations that could result from measurement errors or minor inconsistencies in the data collection process. For each subject and speed, force data was also scaled so that the average peak was equal to the subject's body weight[39] (see Fig. 8).

For all trials performed on the treadmill, heel strike and toe-off events were detected using the already processed force data. The force data was first further smoothed with a moving average filter with a window size of 30 data points. Then, heel strike and toe-off events were found using a threshold of 5% body weight. More specifically, when the total measured filtered force on each belt of the treadmill increased from almost 0 to about 5% of the body weight, it was deemed as a heel-strike event. Similarly, when the total filtered force was reduced from about 5% of body weight to almost 0%, it was deemed as the toe-off event.

For plotting and validation purposes, EMG data was further processed, but this processed data is not included in the available dataset. This process will be outlined so that the figures seen below can be recreated if desired. Muscle activity was recorded and sampled at 2000 *Hz*. It was then bandpass-filtered with a fourth-order Butterworth filter with low and high cutoff frequencies of 30 and 300 *Hz*, respectively. The data then underwent full-wave rectification and the envelope was found using the moving average of the squared data, with a window size of 200 data points. Next, the maximum voluntary contraction (MVC) value was found for each speed, by calculating the 99.9^{th} percentile value of each muscle activation across the entire trial. Then, the data was low-pass filtered with a fourth-order Butterworth filter with a cutoff frequency of 5 *Hz*, before scaling it using the MVC per muscle across each trial. The average inter-participant muscle activation profiles for the middle speed (0.8 m/s) are presented in Fig. 9. It should be noted that no outliers have been removed from the provided data. However, outliers were removed for plotting purposes.

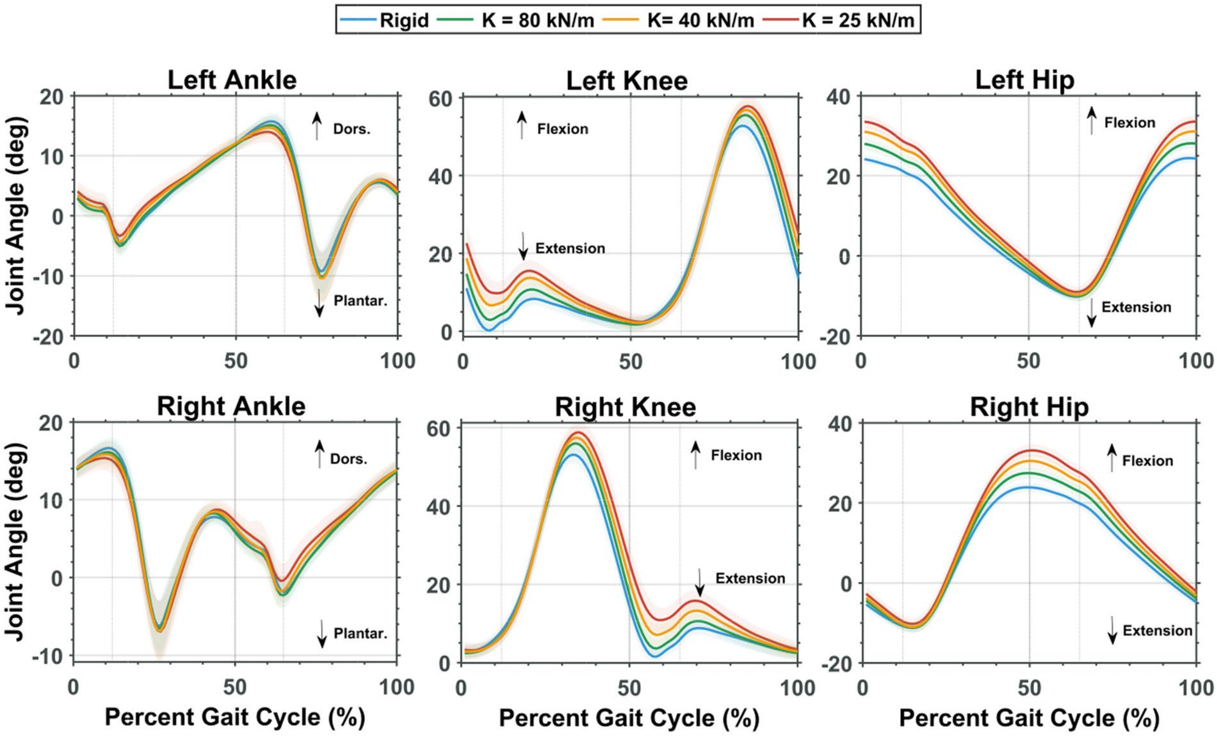

Fig. 4 Mean inter-participant kinematic profiles of left and right lower limbs during a single trial (trial 1: speed 0.8 m/s) across different stiffness levels. Solid lines and shaded regions represent the average trajectory and its variation within one standard deviation, respectively. Gait cycles begin (0%) and end (100%) at left heel strike (LHS).

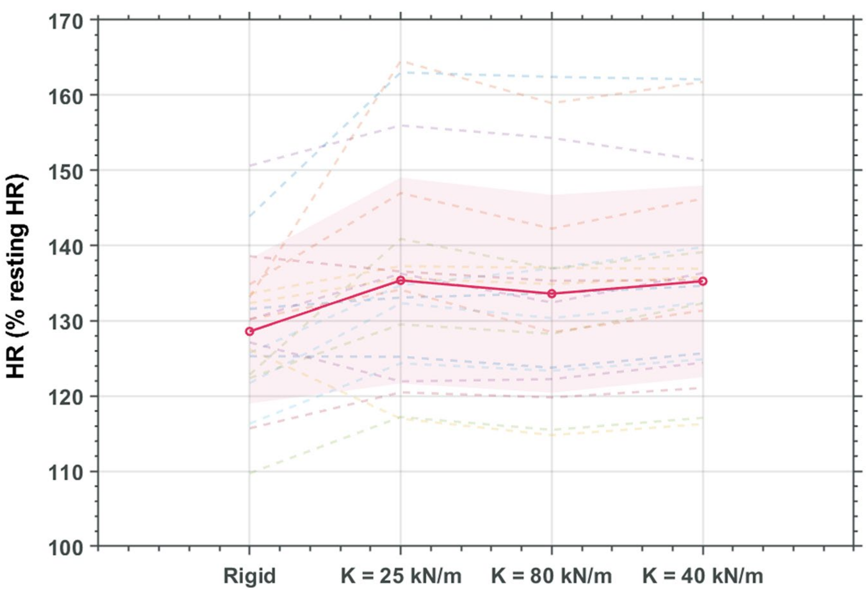

Fig. 5 Mean inter-participant heart rate (HR) data per stiffness condition (horizontal axis) is shown as a solid line. Each dashed line represents the average heart rate per condition for each single subject throughout a single trial (trial 1 = 0.8 m/s). The shaded region represents the variation within one standard deviation of heart rate across all participants per condition. Normalization is with respect to each participant's resting heart rate.

Data Records

The dataset is openly available and can be accessed using Figshare[40]. The data is formatted as separate MATLAB structures for each participant. Each structure per participant is coded as *SUBXX*, where XX represents the participant ID as listed in Table 1. The anthropometric and demographic information in Table 1 are also included in the provided data structures as *SUBXXX.subjectInfo*. For each participant, the data is separated into three trials,

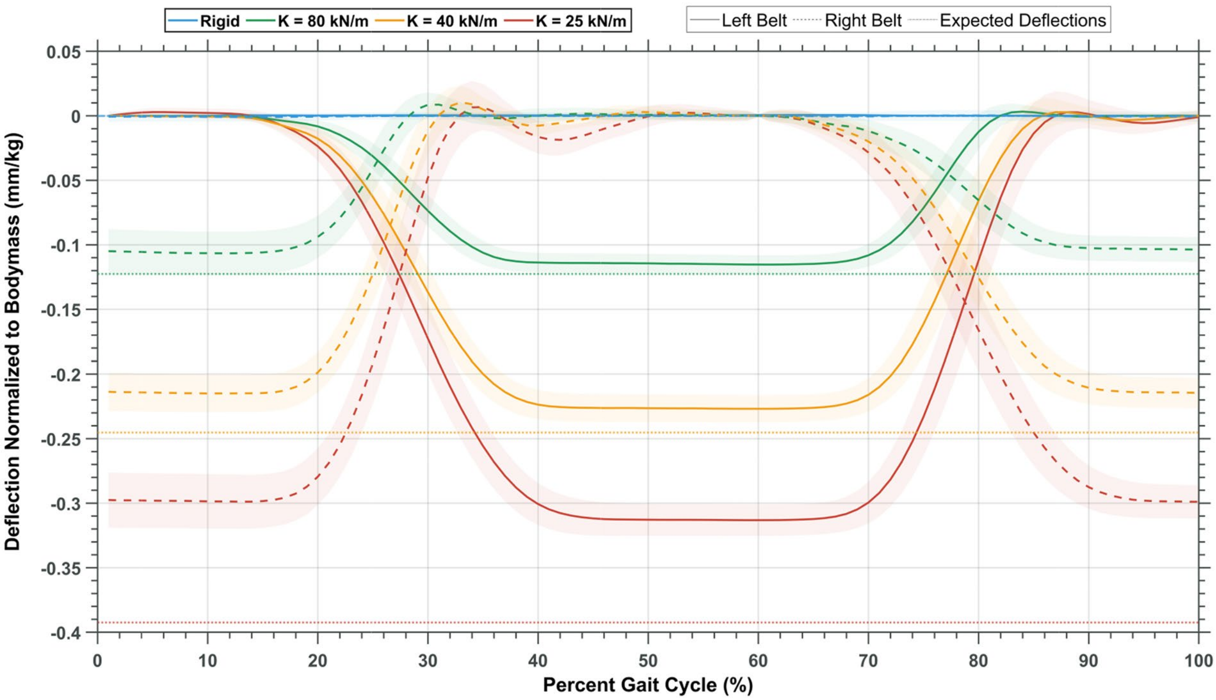

Fig. 6 Average deflection of the left (solid) and right (dashed) VST 2 belts across participants. Deflection is normalized to participant bodymass. The dotted lines represent the expected deflection normalized to bodymass (NBD) for each stiffness condition. Gait cycles begin (0%) and end (100%) at left heel strike (LHS).

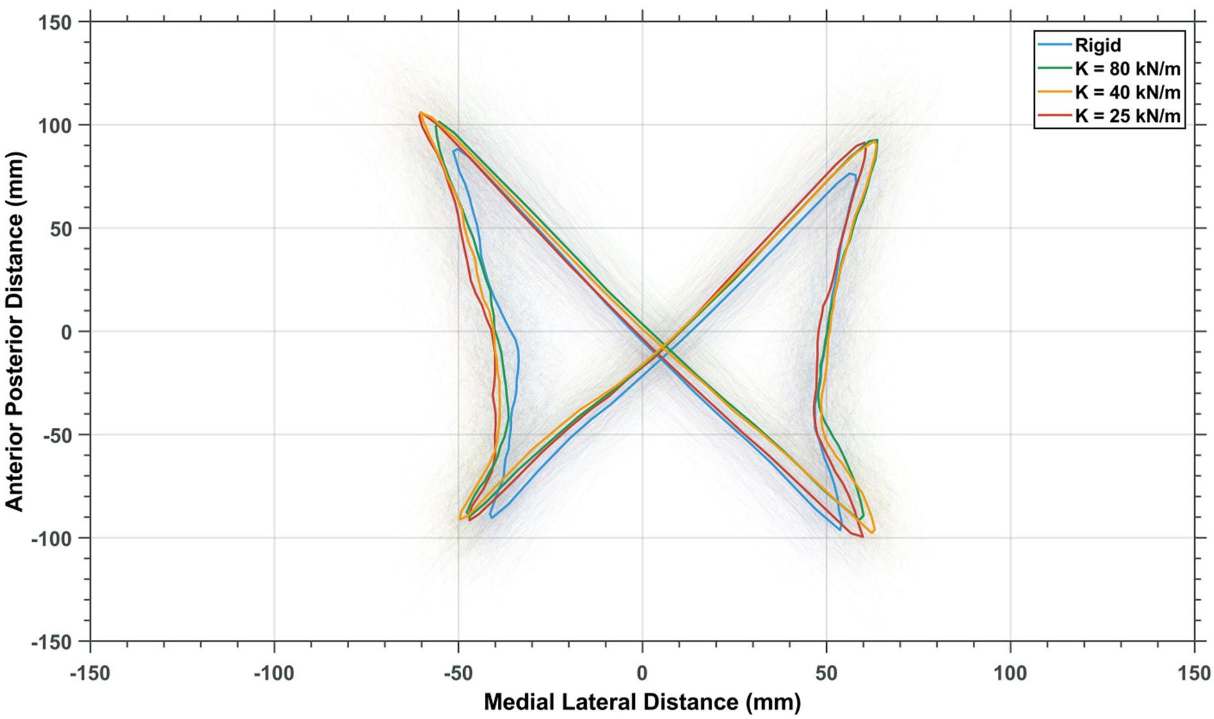

Fig. 7 The center of pressure (CoP) data with respect to the Center of Mass (CoM) for a representative participant during a single trial (trial 1: speed 0.8 m/s). The CoP is normalized using the CoM calculated by Vicon Nexus with the Plug-In Gait model. This is achieved by subtracting the CoM in the x and y directions from the CoP since both are recorded with respect to the same coordinate frame. The solid lines represent the average CoP profile per condition, while the transparent background lines show the CoP trajectory during all gait cycles of each condition.

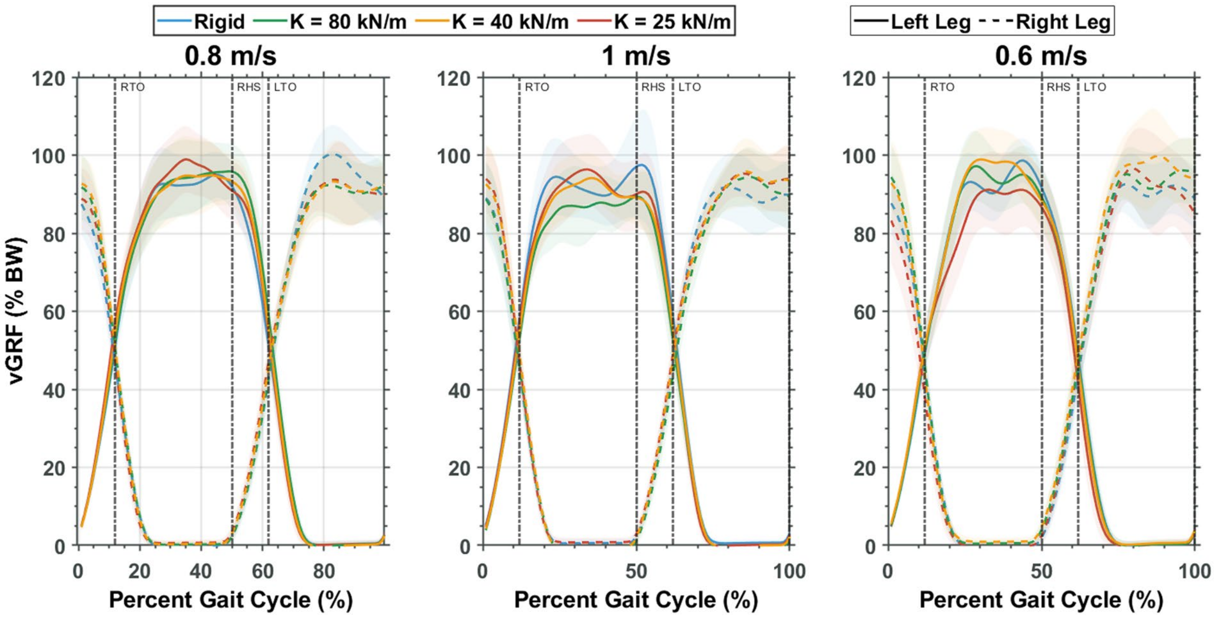

Fig. 8 Vertical Ground Reaction Force (vGRF) profile of the left (solid) and right (dashed) lower limbs for a representative participant across all speeds. Gait cycles begin (0%) and end (100%) at left heel strike (LHS). The major gait events are marked with dotted lines (Right Toe Off (RTO), Right Heel Strike (RHS), Left Toe Off (LTO)).

each one corresponding to a different speed (*speed0p8: 0.8 m/s, speed1p0: 1 m/s, speed0p6: 0.6 m/s*). Each trial consists of the four stiffness conditions that were tested (K = 1000 kN/m, K = 25 kN/m, K = 80 kN/m, K = 40 kN/m), and for each of the tested conditions, the data provided follows the structure presented in Tables 3, 4, 5, and 6. Further documentation for the dataset can be found in the corresponding README file.

Technical Validation

To the best of the authors knowledge, this is the first public dataset to include participants walking over compliant terrain. Compared to previous works, this dataset also has a relatively large number of subjects and hours of data collected. Contained are approximately 18 hours of total data, rendering it relevant even for statistical models and machine learning algorithms.

VST 2 Stiffness and Deflection. VST 2 stiffness accuracy can be evaluated using known load on the treadmill and measuring the resulted deflection. VST 2 stiffness and deflection data was collected using C++ applications that utilize shared memory processes that keep transmission lag minimal. In addition, treadmill platform deflection is given through optical motion capture, as with the marker data, maximizing accuracy of deflection values to the motion capture calibration. The amount of data drop was also very low, with less than 0.1 percent of relevant frames being dropped. The platform effective stiffness was calibrated using an average subject in terms of weight (80 kg) walking on VST 2, and observing the platform deflection. Stiffness values were then calculated and set as the calibration stiffnesses. This ensures the expected and consistent deflection on the two belts during a single stance, within the range of subject weights that participated in the study (see Table 2).

Motion Capture Data. Motion capture data was collected using an optical marker-based motion capture system (Vicon Motion Systems Ltd.), as opposed to other datasets that use Inertial Measurement Units (IMU) only. Optical motion capture is the gold standard for gait analysis, with very strong test-retest and inter-tester reliability in all three anatomical planes[41]. The Vicon camera system has an accuracy of a system error lower than 2.0mm[42], with the system calibration showing 0.25mm or less for the camera error, which is well within the expected range.

Muscle Activity Data (EMG). Muscle activity was collected with Delsys Trigno wireless surface electromyography (EMG) electrodes (Delsys Inc.), which reduce unneeded cable tension. Sensors were applied to alcohol-wiped, dry, shaved skin. Muscles were contracted at each sensor placement to ensure a viable location was found, and a low signal-noise ratio was retained. Normalization consisted of using the peak dynamic method[43], which has been shown to reduce inter-subject variability when comparisons relative to individual muscle effort are not desired.

Force Data. Vertical ground reaction force measurements were collected with force mats (TekScan 3140 with VersaTek Cuffs, TekScan Inc.), allowing full body kinetics to be estimated as opposed to other works that do not include force measurements. Participants were only allowed to wear socks during the walking trials, ensuring

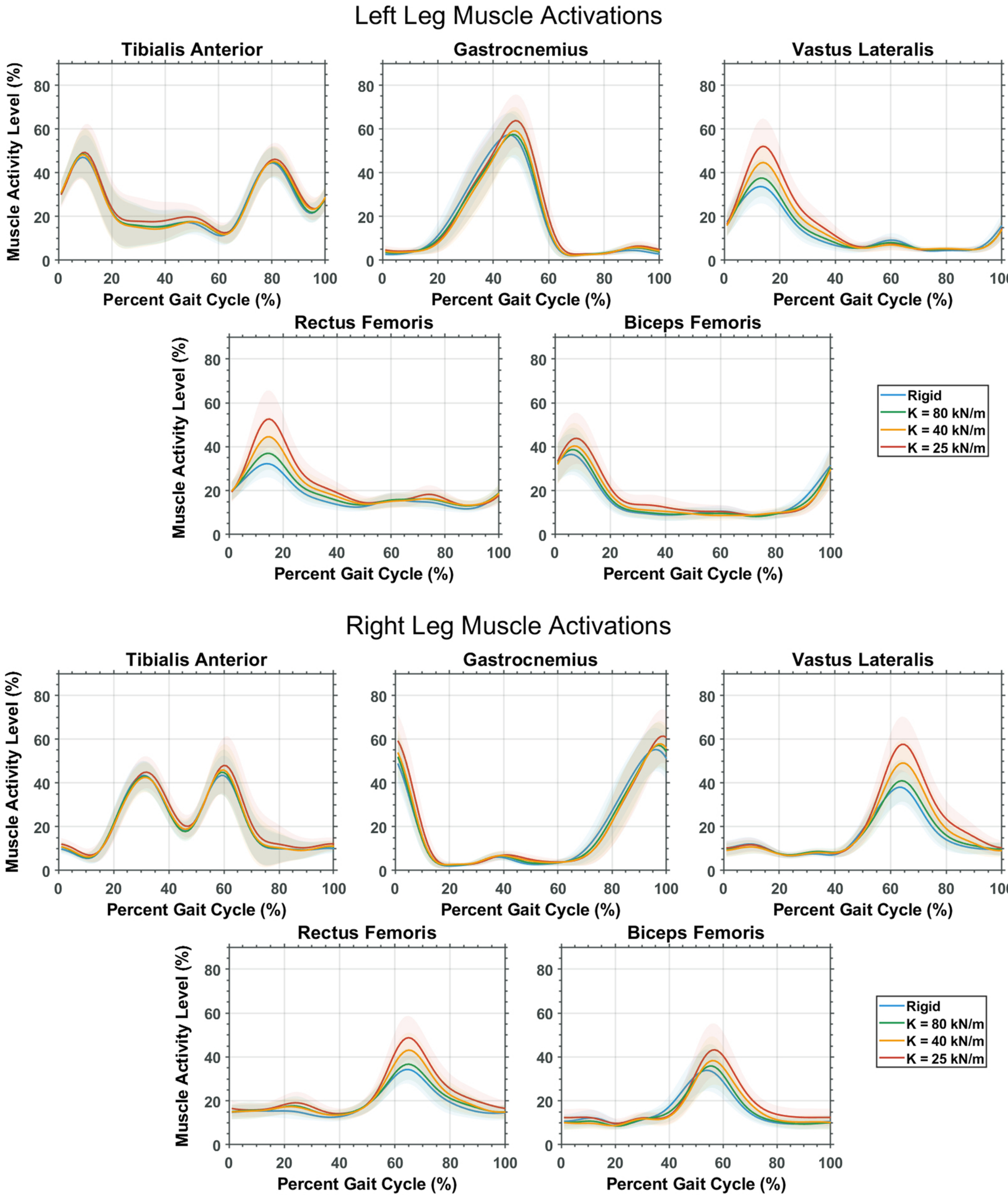

Fig. 9 Mean inter-participant muscle activation profiles of left and right lower limbs during a single trial (trial 1: speed 0.8 m/s). Solid lines and shaded regions represent the average profile and its variation within one standard deviation, respectively. Gait cycles begin (0%) and end (100%) at left heel strike (LHS).

stiffness at the foot is controlled, and CoP is not affected by different shoe sole patterns. The high spatial resolution (1 *cm*) of these force mats allows for highly accurate measurements of the CoP and vertical force.

Data Collection. During data collection, several measures were taken to ensure data quality. Subject preparation was standardized, with one trained and experienced primary experimenter placing all marker and EMG sensors with double-sided tape to ensure the precision of anatomical landmarks between subjects, following accepted standard guidelines[44]. Markers were put on the skin wherever possible or on tight-fitting clothes, according to the documentation from Vicon. Markers did not fall off during any of the trials. Joint kinematics were calculated

Field within structure	Unit	Sampling frequency	Contents
time.time	sec	—	Time of experiment.
			Array format: (total frames x 1)
			1st Dimension: Frames of gait cycle
			2nd Dimension: time
hr.hr	bpm	100 Hz	Heart rate data
			Array format: (total frames x 1)
			1st Dimension: Frames of gait cycle
			2nd Dimension: heart rate
gaitEvents.(gaitEvent)	sec	—	Timing of gait events
			Array format: (total frames x 1)
			1st Dimension: Frames of gait cycle
			2nd Dimension: gait event time

Table 3. Description of data fields within each participant structure. This table includes data that does not fall under the category of kinematic, kinetic, or EMG data.

Field within structure	Unit	Sampling frequency	Contents
markers.(markerName)	mm	100 Hz	Position in the coordinate frame of the markers as shown in Fig. 1
			Array format: (total frames x 3)
			1st Dimension: Frames of gait cycle
			2nd Dimension: x/y/z position in global frame
jointAngles.(jointName)	deg	100 Hz	Full body joint angles as defined in VICON's Full Body Plug in Gait model.
			Array format: (total frames x 3)
			1st Dimension: Frames of gait cycle
			2nd Dimension: x/y/z rotation in local frame
jointForces.(jointName)	N/kg	100 Hz	Force vectors acting on the joint angles, given in the more distal segment's frame of reference.
			Array format: (total frames x 3)
			1st Dimension: Frames of gait cycle
			2nd Dimension: x/y/z joint force
jointMoments.(jointName)	N.m/kg	100 Hz	Full body joint angle moments normalized by the participant's bodymass.
			Array format: (total frames x 3)
			1st Dimension: Frames of gait cycle
			2nd Dimension: x/y/z joint moments
jointPowers.(jointName)	W/kg	100 Hz	Estimated power at each joint expressed as as a single number (scalar).
			Array format: (total frames x 1)
			1st Dimension: Frames of gait cycle
			2nd Dimension: joint power
CoM.CoM	mm	100 Hz	Center of Mass (CoM) in the x, y, and z global frame as calculated by VICON Nexus.
			Array format: (total frames x 3)
			1st Dimension: Frames of gait cycle
			2nd Dimension: CoM_x, CoM_y, CoM_z

Table 4. Description of data fields within each participant structure. This table includes all data that was sampled at 100 Hz.

with the Vicon Plug-In Gait full-body model, which has been shown to have high reliability (ICC > 0.76-90)[45,46] (see Fig. 4). Trials were restarted if a full, complete trial was not attained, keeping consistency between subjects.

Data Processing. All data were processed using well-established filtering and normalization techniques and were checked visually and manually through all processing steps. Gap filling was minimized, but used with known established methods inside the Vicon Nexus software, and was completed before any other pre-processing steps. Joint origin frames were inspected for each subject, with adjustments made before data export to ensure accurate kinematics even further in case marker placement was not satisfactory. Temporal gait parameters are reported, similarly to other works. Foot-contact events are determined by the most accurate kinematic-based detection algorithm[17] in real-time, with offline events calculated using GRF data.

The recorded magnitudes of all sensors and variables were within expected ranges, and distributions of variables were visually inspected with graphs and tables to ensure high quality (see Figs. 4, 5, 6, 7, 8, and 9). This dataset correlated well with other datasets containing gait parameters[47–49].

Field within structure	Unit	Sampling frequency	Contents
EMG.(EMGName)	V	2000 Hz	Muscle activity data as measured by the wireless Delsys Trigno sensors.
			Array format: (total frames x 1)
			1st Dimension: Frames of gait cycle
			2nd Dimension: muscle activation
imuAcc.(EMGName)	mm/s^2	2000 Hz	Accelerometer data from the onboard IMU of the wireless Delsys Trigno sensors.
			Array format: (total frames x 1)
			1st Dimension: Frames of gait cycle
			2nd Dimension: x/y/z acceleration
imuGyro.(EMGName)	deg/s	2000 Hz	Gyroscopic data from the onboard IMU of the wireless Delsys Trigno sensors.
			Array format: (total frames x 1)
			1st Dimension: Frames of gait cycle
			2nd Dimension: x/y/z angular velocity

Table 5. Description of data fields within each participant structure. This table includes all data that was sampled at 2000 Hz.

Field within structure	Unit	Sampling frequency	Contents
GRF.GRF	electrical signal	65 Hz	Vertical Ground Reaction Forces (vGRF) from the force mats embedded underneath the two belts of VST 2.
			Array format: (total frames x 2)
			1st Dimension: Frames of gait cycle
			2nd Dimension: left vGRF, right vGRF
CoP.CoP	mm	65 Hz	Center of Pressure (CoP) from the force mats embedded underneath the two belts of VST 2.
			Array format: (total frames x 2)
			1st Dimension: Frames of gait cycle
			2nd Dimension: CoP_x, CoP_y

Table 6. Description of data fields within each participant structure. This table includes all data that was sampled at 65 Hz.

Limitations. Some limitations of this dataset include the lack of diversity in the subjects. All subjects were healthy, young adults, limiting the generalizability of the dataset to other populations, such as the elderly or individuals with mobility impairments. In addition, the data contains drift in GRF data, which is a known limitation of the equipment used. However, drift was estimated to be less than 1% of the total force, and was corrected for in post-processing. The force mats are piezo-electrical sensors, so there exists a known tradeoff between aggregate compressed time and decompressed time. Researchers using this dataset should implement one of the many known robust drift correction algorithms[50]. Additional limitations of the dataset include the use of only task-specific EMG scaling, without isometric or dynamic Maximum Voluntary Contraction (MVC) measurements, which may limit the interpretability of the EMG data. The kinetic measurement frequency of 65 Hz, while adequate for basic gait analysis, may reduce the precision of event detection and the synchronization of multimodal data streams. Furthermore, the absence of data on self-selected comfortable walking speeds limits the generalizability of the findings to more natural walking conditions, while the lack of randomization in the speed and stiffness conditions across the participants should be noted.

Usage Notes

Our dataset includes a README file, which provides more detailed documentation on the provided data structure. Included is also a MATLAB script titled *exampleScript.m*, which provides an overview of how to quickly access and plot different types of data within the MATLAB structure. The code indicates how to load a single or the full list of participant data into the MATLAB workspace and then plot the desired variables. The user needs to manually define the fields they wish to access according to the dataset structure described in Tables 3, 4, 5, and 6, as well as the README file.

Additionally, three helper MATLAB functions are included with this dataset to aid with data processing and handling. The function *processGRF.m* can be used to filter and scale the raw GRF data provided in this dataset. The filtering uses a moving average filter with a window size of 60 data points. For each participant, speed, and stiffness condition and assuming a double peak profile of the vertical GRF, force data is scaled so that the average value of the peaks is equal to the participant's body weight[39]. It should be noted that this is a helper function that resembles the processing followed to extract the GRF figures in this paper (see Fig. 8). The GRF data provided in this dataset is in its raw form, so the helper function can be used to transform the raw GRF data into Newtons (N).

The function *processEMG.m* can be used to filter and scale the raw EMG data provided in this dataset. It should be noted that this is a helper function that follows the processing steps used to analyze the EMG data presented in this paper (see Fig. 9). The raw EMG data provided in this dataset can be processed using this function, facilitating further analysis.

Finally, the function *timeseriesConvert.m* can be used to convert gait cycle data into continuous time-series data. The function takes the discrete gait cycle data and concatenates them to reconstruct a continuous representation of the walking signal. This is useful for researchers interested in studying human gait dynamics and implementing models that require unprocessed continuous data.

It should be noted that using these helper functions is not mandatory; they represent the authors' chosen method for processing and handling data. Users are free to utilize their own preferred approaches that best suit their specific applications.

Code availability

The dataset and sample code scripts to access, process, and plot the data can be found on Figshare[40]. The data is provided as 20 MATLAB structures, one for each participant's data. Additionally, an example script and three helper functions are included to assist with accessing, plotting, and processing the provided data. Detailed documentation about the provided data architecture can be found in the README file included in Figshare[40]. A video presentation of the experimental protocol is also included with the dataset files in the Figshare repository[40].

Received: 11 October 2024; Accepted: 6 January 2025;
Published online: 16 January 2025

References

1. Hobbs, B. & Artemiadis, P. A Review of Robot-Assisted Lower-Limb Stroke Therapy: Unexplored Paths and Future Directions in Gait Rehabilitation. *Frontiers in Neurorobotics* **14**, 19, https://doi.org/10.3389/fnbot.2020.00019 (2020).
2. Hashmi, M. Z. U. H., Riaz, Q., Hussain, M. & Shahzad, M. What Lies Beneath One's Feet? Terrain Classification Using Inertial Data of Human Walk. *Applied Sciences* **9**, 3099, https://doi.org/10.3390/app9153099 (2019).
3. Chang, M. D., Sejdić, E., Wright, V. & Chau, T. Measures of dynamic stability: Detecting differences between walking overground and on a compliant surface. *Human Movement Science* **29**, 977–986, https://doi.org/10.1016/j.humov.2010.04.009 (2010).
4. MacLellan, M. J. & Patla, A. E. Adaptations of walking pattern on a compliant surface to regulate dynamic stability. *Experimental Brain Research* **173**, 521–530, https://doi.org/10.1007/s00221-006-0399-5 (2006).
5. Marigold, D. S. & Patla, A. E. Adapting Locomotion to Different Surface Compliances: Neuromuscular Responses and Changes in Movement Dynamics. *Journal of Neurophysiology* **94**, 1733–1750, https://doi.org/10.1152/jn.00019.2005 (2005).
6. Hafner, B. J., Morgan, S. J., Abrahamson, D. C. & Amtmann, D. Characterizing mobility from the prosthetic limb user's perspective: Use of focus groups to guide development of the Prosthetic Limb Users Survey of Mobility. *Prosthetics and Orthotics International* **40**, 582–590, https://doi.org/10.1177/0309364615579315 (2016).
7. Hawkins, K. A., Clark, D. J., Balasubramanian, C. K. & Fox, E. J. Walking on uneven terrain in healthy adults and the implications for people after stroke HHS Public Access. *NeuroRehabilitation* **41**, 765–774, https://doi.org/10.3233/NRE-172154 (2017).
8. Kim, J., Major, M. J., Hafner, B. & Sawers, A. Frequency and Circumstances of Falls Reported by Ambulatory Unilateral Lower Limb Prosthesis Users: A Secondary Analysis. *PM&R* **11**, 344–353, https://doi.org/10.1016/J.PMRJ.2018.08.385 (2019).
9. Miller, W. C., Speechley, M. & Deathe, B. The prevalence and risk factors of falling and fear of falling among lower extremity amputees. *Archives of Physical Medicine and Rehabilitation* **82**, 1031–1037, https://doi.org/10.1053/apmr.2001.24295 (2001).
10. Morgan, S. J., Hafner, B. J. & Kelly, V. E. Dual-task walking over a compliant foam surface: A comparison of people with transfemoral amputation and controls. *Gait & Posture* **58**, 41–45, https://doi.org/10.1016/j.gaitpost.2017.07.033 (2017).
11. Arifin, N., Osman, N. A. A., Ali, S., Gholizadeh, H. & Abas, W. A. B. W. Postural stability characteristics of transtibial amputees wearing different prosthetic foot types when standing on various support surfaces. *The Scientific World Journal* **2014**, 856279, https://doi.org/10.1155/2014/856279 (2014).
12. Richardson, J. K., Thies, S. B., DeMott, T. K. & Ashton-Miller, J. A. Gait analysis in a challenging environment differentiates between fallers and nonfallers among older patients with peripheral neuropathy. *Archives of Physical Medicine and Rehabilitation* **86**, 1539–1544, https://doi.org/10.1016/j.apmr.2004.12.032 (2005).
13. McMahon, T. A. & Greene, P. R. The influence of track compliance on running. *Journal of Biomechanics* **12**, 893–904, https://doi.org/10.1016/0021-9290(79)90057-5 (1979).
14. Davies, S. E. H. & Mackinnon, S. N. The energetics of walking on sand and grass at various speeds. *Ergonomics* **49**, 651–660, https://doi.org/10.1080/00140130600558023 (2006).
15. Hennah, C. & Doumas, M. Dual-task walking on real-world surfaces: Adaptive changes in walking speed, step width and step height in young and older adults. *Experimental Gerontology* **177**, 112200, https://doi.org/10.1016/J.EXGER.2023.112200 (2023).
16. Van den Berg, M. E. L., Barr, C. J., McLoughlin, J. V. & Crotty, M. Effect of walking on sand on gait kinematics in individuals with multiple sclerosis. *Multiple Sclerosis and Related Disorders* **16**, 15–21, https://doi.org/10.1016/J.MSARD.2017.05.008 (2017).
17. Karakasis, C., Salati, R. and Artemiadis, P. "Adjusting the Quasi-Stiffness of an Ankle-Foot Prosthesis Improves Walking Stability during Locomotion over Compliant Terrain," in *IEEE International Conference on Intelligent Robots and Systems*, pp. 2140–2145, https://doi.org/10.1109/IROS55552.2023.10342344 (2023).
18. Karakasis, C., "Robust and Stable Locomotion over Compliant Terrains: Application to Lower-limb Prostheses and Bipedal Robots," *PhD thesis, University of Delaware*, (2024).
19. Hobbs, B. and Artemiadis, P. "Virtual Reality-based Robot-Assisted Method for Gait Training Showing Retention of Anticipatory Motor Responses," in *10th IEEE RAS/EMBS International Conference on Biomedical Robotics and Biomechatronics (BioRob)*, (2024).
20. Angelidou, C. & Artemiadis, P. On Predicting Transitions to Compliant Surfaces in Human Gait via Neural and Kinematic Signals. *IEEE Transactions on Neural Systems and Rehabilitation Engineering* **31**, 2214–2223, https://doi.org/10.1109/TNSRE.2023.3272355 (2023).
21. Angelidou, C. and Artemiadis, P. "On Intuitive Control of Ankle-Foot Prostheses: A Sensor Fusion-Based Algorithm for Real-Time Prediction of Transitions to Compliant Surfaces," *2023 IEEE/RSJ International Conference on Intelligent Robots and Systems (IROS)*, pp. 2122-2127, IEEE, https://doi.org/10.1109/IROS55552.2023.10341783 (2023).
22. Chambers, V. & Artemiadis, P. Using robot-assisted stiffness perturbations to evoke aftereffects useful to post-stroke gait rehabilitation. *Frontiers in Robotics* **9**, 1073746, https://doi.org/10.3389/frobt.2022.1073746 (2023).
23. Huang, H., Kuiken, T. A. & Lipschutz, R. D. A strategy for identifying locomotion modes using surface electromyography. *IEEE Transactions on Biomedical Engineering* **56**, 65–73, https://doi.org/10.1109/TBME.2008.2003293 (2009).
24. Cowan, M., Creveling, S., Sullivan, L.M., Gabert, L. and Lenzi, T. "A Unified Controller for Natural Ambulation on Stairs and Level Ground with a Powered Robotic Knee Prosthesis," in *2023 IEEE/RSJ International Conference on Intelligent Robots and Systems (IROS)*, pp. 2146–2151. https://doi.org/10.1109/IROS55552.2023.10341691 (2023).

25. Cortino, R. J., Best, T. K. & Gregg, R. D. Data-Driven Phase-Based Control of a Powered Knee-Ankle Prosthesis for Variable-Incline Stair Ascent and Descent. *IEEE Transactions on Medical Robotics and Bionics* **2023**, 1–1, https://doi.org/10.36227/techrxiv.23818368.v1 (2023).
26. Reznick, E. *et al*. Lower-limb kinematics and kinetics during continuously varying human locomotion. *Scientific Data* **8**, 1–12, https://doi.org/10.1038/s41597-021-01057-9 (2021).
27. Hood, S., Ishmael, M. K., Gunnell, A., Foreman, K. B. & Lenzi, T. A kinematic and kinetic dataset of 18 above-knee amputees walking at various speeds. *Scientific Data* **7**, 1–8, https://doi.org/10.1038/s41597-020-0494-7 (2020).
28. Embry, K. R., Villarreal, D. J., Macaluso, R. L. & Gregg, R. D. Modeling the Kinematics of Human Locomotion over Continuously Varying Speeds and Inclines. *IEEE Transactions on Neural Systems and Rehabilitation Engineering* **26**, 2342–2350, https://doi.org/10.1109/TNSRE.2018.2879570 (2018).
29. Fukuchi, C. A., Fukuchi, R. K. & Duarte, M. A public dataset of overground and treadmill walking kinematics and kinetics in healthy individuals. *PeerJ* **6**, e4640, https://doi.org/10.7717/peerj.4640 (2018).
30. Chambers, V. *et al*. "The Variable Stiffness Treadmill (VST) 2: Development and Validation of a Unique Tool to Investigate Locomotion on Compliant Terrains," *ASME Journal of Mechanisms and Robotics*, https://doi.org/10.1115/1.4066173 (2024).
31. Cho, S. H., Park, J. M. & Kwon, O. Y. Gender differences in three dimensional gait analysis data from 98 healthy Korean adults. *Clinical Biomechanics* **19**, 145–152, https://doi.org/10.1016/j.clinbiomech.2003.10.003 (2004).
32. Vicon Motion Systems, "Plug-in Gait Reference Guide," *Vicon Motion Systems*, Available at: https://help.vicon.com/space/Nexus216/11607059/Plug-in+Gait+Reference+Guide (2021).
33. Hermens, H. J., Freriks, B., Disselhorst-Klug, C. & Rau, G. Development of recommendations for SEMG sensors and sensor placement procedures. *Journal of Electromyography and Kinesiology* **10**, 361–374, https://doi.org/10.1016/s1050-6411(00)00027-4 (2000).
34. Stegeman, D. F., Kleine, B. U., Lapatki, B. G. & Van Dijk, J. P. High-density surface EMG: Techniques and applications at a motor unit level. *Biocybernetics and Biomedical Engineering* **32**, 3–27, https://doi.org/10.1016/S0208-5216(12)70039-6 (2012).
35. Vicon Motion Systems, "Vicon Nexus User Guide," *Vicon Motion Systems*, Available at: https://help.vicon.com/space/Nexus216/11605325/Vicon+Nexus+User+Guide (2021).
36. Barkan, A., Skidmore, J. and Artemiadis, P. "Variable Stiffness Treadmill (VST): A novel tool for the investigation of gait," *2014 IEEE International Conference on Robotics and Automation (ICRA)*, pp. 2838-2843, https://doi.org/10.1109/ICRA.2014.6907266 (2014).
37. Skidmore, J., Barkan, A. & Artemiadis, P. Variable Stiffness Treadmill (VST): System Development, Characterization, and Preliminary Experiments. *IEEE/ASME Transactions on Mechatronics* **20**, 1717–1724, https://doi.org/10.1109/TMECH.2014.2350456 (2015).
38. Capó-Lugo, C. E., Mullens, C. H. & Brown, D. A. Maximum walking speeds obtained using treadmill and overground robot system in persons with post-stroke hemiplegia. *Journal of NeuroEngineering and Rehabilitation* **9**, 1–14, https://doi.org/10.1186/1743-0003-9-80/FIGURES/3 (2012).
39. Perry, J. "Gait Analysis: Normal and Pathological Function," *SLACK Incorporated*, pp. 414-417, (2010).
40. Angelidou, C., Chambers, V., Hobbs, B., Karakasis, C. and Artemiadis, P. "Kinematics, kinetics, and muscle activations during human locomotion over compliant terrains," https://doi.org/10.6084/m9.figshare.27180288 (2024).
41. Van Criekinge, T. *et al*. A full-body motion capture gait dataset of 138 able-bodied adults across the life span and 50 stroke survivors. *Scientific Data* **10**, 852, https://doi.org/10.1038/s41597-023-02767-y (2023).
42. Merriaux, P., Dupuis, Y., Boutteau, R., Vasseur, P. & Savatier, X. A study of vicon system positioning performance. *Sensors* **17**, 1591, https://doi.org/10.3390/s17071591 (2017).
43. Burden, A. How should we normalize electromyograms obtained from healthy participants? What we have learned from over 25 years of research. *Journal of Electromyography and Kinesiology* **20**, 1023–1035, https://doi.org/10.1016/j.jelekin.2010.07.004 (2010).
44. Pinto-Fernández, D., Rodriguez-Cianca, D., Juan, C. M. & Torricelli, D. Human Locomotion Databases: A Systematic Review. *IEEE Journal of Biomedical and Health Informatics* **28**, 1716–1729, https://doi.org/10.1109/JBHI.2023.3311677 (2024).
45. Molina-Rueda, F. *et al*. Test–Retest Reliability of a Conventional Gait Model for Registering Joint Angles during Initial Contact and Toe-Off in Healthy Subjects. *International Journal of Environmental Research and Public Health* **18**, 1343, https://doi.org/10.3390/ijerph18031343 (2021).
46. Kainz, H. *et al*. Reliability of four models for clinical gait analysis. *Gait & Posture* **54**, 325–331, https://doi.org/10.1016/j.gaitpost.2017.04.001 (2017).
47. Bovi, G., Rabuffetti, M., Mazzoleni, P. & Ferrarin, M. A multiple-task gait analysis approach: kinematic, kinetic and EMG reference data for healthy young and adult subjects. *Gait & Posture* **33**, 6–13, https://doi.org/10.1016/j.gaitpost.2010.08.009 (2011).
48. Hu, B., Rouse, E. & Hargrove, L. Benchmark datasets for bilateral lower-limb neuromechanical signals from wearable sensors during unassisted locomotion in able-bodied individuals. *Frontiers in Robotics and AI* **5**, 14, https://doi.org/10.3389/frobt.2018.00014 (2018).
49. Camargo, J., Ramanathan, A., Flanagan, W. & Young, A. A comprehensive, open-source dataset of lower limb biomechanics in multiple conditions of stairs, ramps, and level-ground ambulation and transitions. *Journal of Biomechanics* **119**, 110320, https://doi.org/10.1016/j.jbiomech.2021.110320 (2021).
50. Dang, B., Wang, C., Liu, C., Yang, L. and Zhao, Y. "Real-time Baseline Drift Correction Method for Transient Electromagnetic Logging Signals Based on Adaptive Segmentation," *2022 4th International Conference on Intelligent Control, Measurement and Signal Processing (ICMSP)*, pp. 259-262, https://doi.org/10.1109/ICMSP55950.2022.9858940 (2022).

Acknowledgements

This material is based upon work supported by the National Science Foundation under Grants No. 2020009, 2015786, 2025797, and 2018905 and work supported by the National Institutes of Health Grant No. 1R01HD111071-01.

Author contributions

C.A. drafted the first manuscript of this article and coordinated the manuscript with all co-authors. C.A. and V.C. recruited participants, collected measurements, post-processed all data, and analyzed the results. V.C. and B.H. developed the code for data processing and synchronization. B.H. resolved hardware challenges and provided technical support during collection. C.K., B.H., and V.C. developed and integrated the software and the hardware for VST 2. P.A. conceived the work, developed the research agenda behind this work, raised the funding for this research, and supervised all aspects. All authors contributed to the study design, interpreted the results, wrote and revised manuscript sections, read and approved the submitted version.

Competing interests

The authors declare no competing interests.

Additional information

Correspondence and requests for materials should be addressed to P.A.

Reprints and permissions information is available at www.nature.com/reprints.

Publisher's note Springer Nature remains neutral with regard to jurisdictional claims in published maps and institutional affiliations.

Open Access This article is licensed under a Creative Commons Attribution-NonCommercial-NoDerivatives 4.0 International License, which permits any non-commercial use, sharing, distribution and reproduction in any medium or format, as long as you give appropriate credit to the original author(s) and the source, provide a link to the Creative Commons licence, and indicate if you modified the licensed material. You do not have permission under this licence to share adapted material derived from this article or parts of it. The images or other third party material in this article are included in the article's Creative Commons licence, unless indicated otherwise in a credit line to the material. If material is not included in the article's Creative Commons licence and your intended use is not permitted by statutory regulation or exceeds the permitted use, you will need to obtain permission directly from the copyright holder. To view a copy of this licence, visit http://creativecommons.org/licenses/by-nc-nd/4.0/.

© The Author(s) 2025